



Regular article

# In-situ TEM study of dislocation emission associated with austenite growth



Juan Du<sup>a</sup>, Frédéric Momprou<sup>b</sup>, Wen-Zheng Zhang<sup>a,\*</sup>

<sup>a</sup> Key Laboratory of Advanced Materials (MOE), School of Materials Science and Engineering, Tsinghua University, Beijing 100084, PR China

<sup>b</sup> CEMES-CNRS, Université de Toulouse, 29 rue J. Marvig, 31055 Toulouse, France

## ARTICLE INFO

### Article history:

Received 8 September 2017

Accepted 9 October 2017

Available online xxxx

### Keywords:

In-situ TEM

Dislocation emission

Pitsch OR

Austenite/ferrite interface

## ABSTRACT

The emission of dislocations from the tip of a newly transformed austenite lath, with a near Pitsch orientation relationship with the ferrite matrix, was observed at 760 °C in a duplex stainless steel, using in-situ transmission electron microscopy. The dynamics of dislocation loops with  $[111]_b/2$  Burgers vector were carefully analyzed. An estimation of stress concentration at the tip was made using dislocations as stress probes. These real-time observations verify directly for the first time that dislocation activity assists the growth of austenite precipitates, and provide quantitative data for revealing the stress field generated by interface migration.

© 2017 Published by Elsevier Ltd on behalf of Acta Materialia Inc.

The phase transformation between austenite (fcc) and ferrite (bcc) is one of the most important solid-state transformations because of its practical importance as a metallurgical tool to tailor the mechanical properties of steels. A fundamental step to understand the phase transformation is to study interfacial structures between product and matrix phases. Although numerous experimental and theoretical studies have been made on the structure of fcc/bcc interfaces [1–13], only few in-situ experiments have been conducted to directly observe the interface migration [14,15]. There are considerable and persuasive evidence that the phase transformation is frequently associated with dislocation activity, especially when the product phase exhibits a plate, lath or needle shape. It has been reported that matrix dislocations connect with growth ledges in a Ni–Cr-alloy [1,16,17] and that matrix dislocations interconnect precipitate needles throughout the matrix in a Fe–Cu alloy [2]. An in-situ transmission electron microscopy (TEM) study has revealed the emission of dislocations both in austenite and ferrite to release stress near the transformation front during the decomposition of Fe–C austenite [15]. However, the details of dislocation activity associated with the moving interface remain unclear, and a complete dislocation characterization is still lacking in the previous work. The dislocation activity is probably due to a long-range stress field caused by the phase transformation. Therefore, a detailed description of the dislocation activity may shed some light on this stress field, which is often uneasy to measure quantitatively.

In this study, we carried out in-situ TEM experiments to observe directly growth of fresh austenite from ferrite matrix in a duplex stainless steel, and tracked dislocation activity associated with the interface migration. Fe–24.9Cr–7.0Ni–3.1Mo (wt%) alloy was used in the present work. 10 mm × 10 mm × 10 mm alloy blocks were encapsulated in silica tubes for a solution treatment at 1300 °C for 30 min, followed by water quenching so that ferrite phase could be preserved at room temperature. TEM sample preparation was obtained by mechanical thinning and twin-jet polishing (with an electrolyte of 8 vol% perchloric acid in ethanol at –30 °C and with an applied voltage of 20 V). In-situ TEM experiments were performed in a Philips CM20FEG microscope operated at 200 kV using a GATAN heating holder. Samples were heated first at the highest temperature rate (several °C/s) up to 700 °C, and then slowly heated by 5 °C increments until the first fresh austenite was noticed. The interface motions were recorded using a Gatan Orius side entry camera operated at 15 fps. After in-situ experiments, crystallographic features were determined by a Kikuchi line analysis, with an average misorientation error of ±0.5°. All crystallographic indexes are self-consistent with a selected variant of the orientation relationship (OR).

Upon heating, fresh austenite precipitates are formed by nucleation and growth from the ferrite matrix. As in bulk materials, the fresh austenite in thin TEM foils also exhibits a lath morphology, with the long axis lying approximately in the foil. The observations reported below focus on the phenomena of growth close to the moving tip.

Fig. 1 shows a series of bright field images extracted from a video sequence (see Supplementary movie S1) taken at 760 °C, with the time for Fig. 1a being arbitrarily set at  $t = 0$  s. It can be seen from Fig. 1 that besides the foil surfaces the growing austenite lath is enclosed by two near

\* Corresponding author.

E-mail address: [zhangwz@mail.tsinghua.edu.cn](mailto:zhangwz@mail.tsinghua.edu.cn) (W.-Z. Zhang).

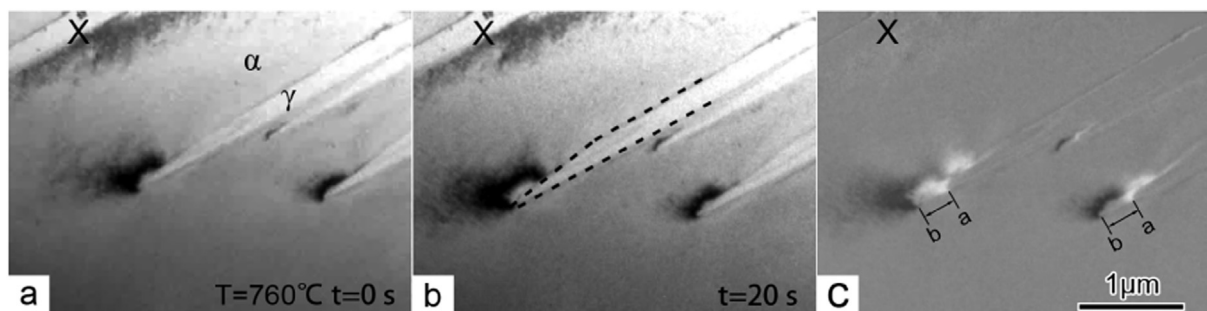


**Fig. 1.** Wedge-shaped tip of austenite ( $\gamma$ ) lath growing in ferrite ( $\alpha$ ) matrix at 760 °C: a)  $t = 0$  s; b)  $t = 20$  s. c) is the image difference a)–b) highlighting the growth of the austenite lath. X is a reference marker. See Supplementary movie S1 for details.

parallel flat interfaces and one inclined interface, resulting in a wedge tip. Using X as a fiducial marker, the overall tip migration along the long axis can be measured from the image difference between Fig. 1a and b, as given in Fig. 1c. An average growing rate of 15.6 nm/s is estimated. A bending contour adjacent to the inclined interface at each tip was observed during the motion. The location of the bending contour suggests an asymmetrical stress field near the migrating tip. For this case, no dislocation activity was observed. A probable reason is that the stress field at the lath tip is below the critical value for dislocation nucleation.

In contrast to the case in Fig. 1, dislocation emission has been observed near the tips of a number of austenite laths. Fig. 2 shows an example of dislocation emission from such a tip. Seventeen dislocation loops were emitted one after another in a similar manner. Fig. 2a–d consist of sequential snapshots (see Supplementary movie S2) of a typical process of the expansion of a dislocation loop at the lath tip. These bright field images were recorded under two-beam condition using  $g_{(011)b}$ . The loop is unclosed, with two ends connecting to two sides of the tip. Once generated, the portion of the loop in the immediate vicinity of the tip does not expand to the matrix immediately, but it apparently hesitates to detach from the tip (as seen from the new small loop in Fig. 2c). After leaving from the tip, the dislocation loop expands rapidly ahead of the tip. It indicates that the emitted dislocation is strongly repelled by the stress field present at the lath tip. When the loop meets the foil surface, it breaks into two dislocation segments that leave a visible trace, due to the presence of a thin oxide layer on the surface. The dislocation meets first the upper surface and then the lower surface, yielding traces  $t_{1u}$  (Fig. 2b) and  $t_{1l}$  (Fig. 2c), respectively. The two dislocation segments, marked by  $s_1$  and  $s_2$  in Fig. 2c, continue to move. While segment  $s_1$  moves away from the tip at a similar rate as the tip-front portion of initial loop, segment  $s_2$  slows down as it moves towards a lath side. After gliding for a certain distance, segment  $s_1$  will cross slip, as evidenced by the change of trace direction (Fig. 2d). The new straight traces on upper and lower surfaces are referred to  $t_{2u}$  and  $t_{2l}$ , respectively. This indicates that  $s_1$  is largely a screw dislocation. Meanwhile, a new dislocation loop was nucleated, as seen in Fig. 2c. In addition to these continuously generated dislocation loops, several other dislocations were occasionally observed in the vicinity of the tip, without being clearly determined. They present a very weak contrast, indicating that they are out of contrast with this diffraction condition.

Post-mortem crystallographic analysis was made on the austenite lath in Fig. 2. The OR between austenite and ferrite was found near the Pitsch OR [18], i.e.,  $(100)_f \parallel (110)_b$ ,  $0.6^\circ$  and  $[0\bar{1}1]_f \parallel [1\bar{1}1]_b$ ,  $0.6^\circ$ , which was seldom observed in steels (the subscript f and b refer to fcc and bcc lattices, respectively). Fig. 2e illustrates schematically the geometry of the austenite lath and the crystallography of several

typical planes of ferrite in Fig. 2a–d. The long axis of austenite lath is  $[\bar{1}7.36.6]_f \parallel [5.16.65.4]_b$ , i.e. lying in the flat interface, with an orientation of  $(0.48\ 0.50\ 0.72)_f \parallel (0.08\ 0.61\ 0.79)_b$ . The measured foil normal is  $(0.85\ 0.38\ 0.36)_b$ . Based on the measured directions of slip traces and widths between traces on the upper and lower surfaces, the slip planes were determined as  $(11\bar{2})_b$  and  $(10\bar{1})_b$ , respectively (see Supplementary materials for the detailed calculation). The Burgers vector of the emitted dislocations is thus determined as the intersection of these two planes, namely  $b = [111]_b/2$ . This result is consistent with the diffraction contrast of the dislocation under  $g_{(011)b}$  in Fig. 2.

In order to analyze the tip motion, a custom made script was used to track the tip position in Fig. 2. To avoid artifacts due to the contrast changes when the dislocations are emitted, the tip motion was analyzed manually by image difference during a short period of time around the dislocation emission. The displacement of the tip along the long axis versus time is given in Fig. 3. The time reference is chosen as the moment of the dislocation being emitted in Fig. 2a. It can be seen from Fig. 3 that the moving rate is almost constant (7–8 nm/s), but with several decelerations shown as kinks on the displacement curve. The change in tip velocity is concomitant with dislocation emission noted by D in Fig. 3. The jerky nature of the tip moving rate is probably due to the accumulation and relaxation of stress field near the tip. The emission of a dislocation loop from the tip may also affect tip moving rate via interaction between the local dislocation loop and the possible interfacial dislocations in the semicoherent interface surrounding the tip. Consequently, the tip halted temporarily. It has been checked that the length and width of austenite lath in Fig. 1 are both smaller than those in Fig. 2, and the foil containing the lath in Fig. 1 is also thinner. In this sense, though the austenite lath in Fig. 1 shares a similar OR with that in Fig. 2, the stress accumulated near the tip could be smaller. This might be a reason why the growth of the small laths in Fig. 1 is not associated with dislocation activity.

Dynamics of dislocations can be explained according to an analysis of dislocation displacement. Fig. 4 shows image differences at difference time intervals between snapshots extracted from the video (see Supplementary movie S2). Dislocations numbered D1 to D5 in Fig. 4a–d show white and black contrasts before and after. Accordingly, the displacement between white and black contrasts can be used to estimate the average moving rate of dislocations. The net shear stress acting on each dislocation results from a combination of the stress field at the lath tip ( $\tau_{tip}$ ), the image stress tending to attract the dislocation loop to the surface ( $\tau_{image}$ ), the line tension ( $\tau_l$ ) and the interaction stress between dislocations ( $\tau_{inter}$ ). As can be seen from Fig. 4a, dislocation D1 moves first rapidly mainly due to the  $\tau_{tip}$  and crosses a zone about 200 nm ahead of the tip. The shear stress required to nucleate the loop can be evaluated by measuring the loop size at the critical configuration before loop expansion, i.e. when  $\tau_{tip}$  is comparable to  $\tau_l$  (i.e. neglecting  $\tau_{image}$  and  $\tau_{inter}$ ).

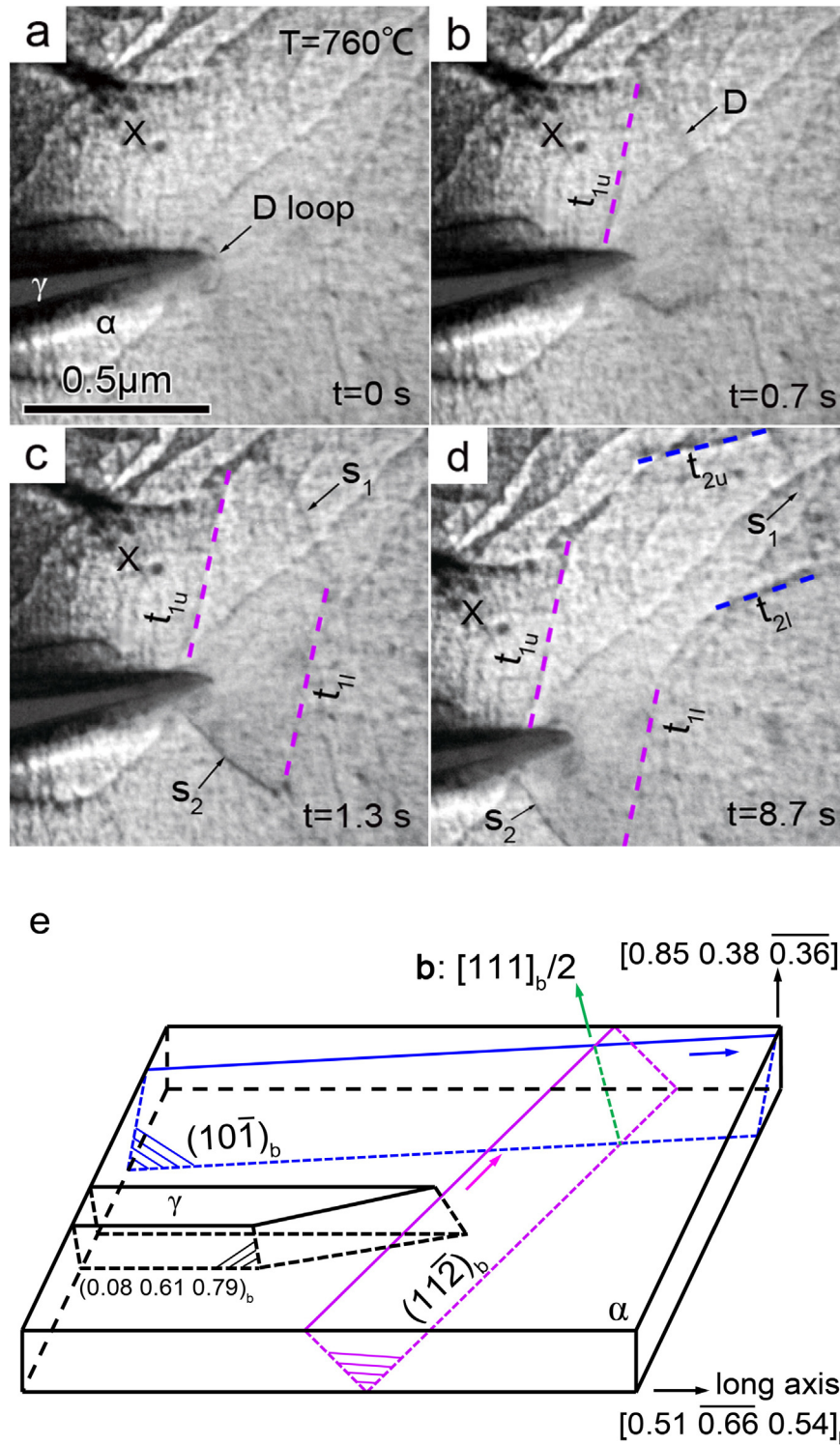


**Fig. 2.** (a–d) In-situ observation of the expansion of a dislocation (D) loop from the tip of an austenite lath. The two sets of dislocation moving traces  $t_1$  and  $t_2$  in the upper surface (u) and lower surface (l) are marked by dashed lines (color online). X is a reference marker. See Supplementary movie S2 for details. (e) Schematic diagram showing the general geometry of austenite lath with ferrite matrix in the foil and two activated slip planes  $(11\bar{2})_b$  and  $(10\bar{1})_b$ .

This can be achieved by calculating the line tension using anisotropic elasticity (DISDI software [19]). Since the critical loop just nucleated is hard to capture, a lower bound of stress can be measured when the loop becomes visible, i.e. few frame before Fig. 2a. An estimation of 170 MPa is retrieved.

A slowly moving pile up is formed 200 nm away from the tip in Fig. 4. In the zone of the pile up, dislocations are almost arranged uniformly. After the rapid motion of D1, the interaction stress pushes all dislocations in the pile up in Fig. 4b away until the net stress acting on D1 decreases. The final position of D1 almost replaces the initial position



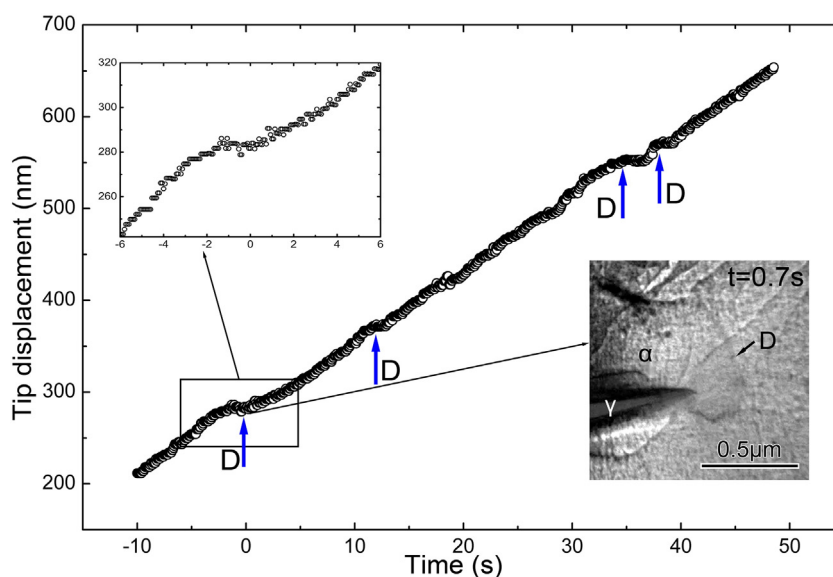


**Fig. 3.** The displacements of the lath tip along the long axis as a function of the transformation time in the time region corresponding to the micrographs in Fig. 2. The blue arrows indicate the emission of a dislocation (D) loop (color online). (For interpretation of the references to color in this figure legend, the reader is referred to the web version of this article.)

of D2. This indicates here that the critical resolved shear stress necessary to move the dislocation is of the order of the interaction stress, which can be estimated as:

$$\tau_{\text{inter}} \approx Gb/2\pi r, \quad (1)$$

where  $G$  is the shear modulus for the alloy,  $b$  is the length of the Burgers vector and  $r$  is the distance between these two dislocations. If we take  $r = 170$  nm (Fig. 4a),  $a_b = 0.2881$  nm (lattice parameter of ferrite) and  $G = 80$  GPa,  $\tau_{\text{inter}}$  is around 19 MPa. These observations indicate that the stress generated at the lath tip decreases rapidly from  $\sim 170$  MPa to 19 MPa over a 200 nm wide region, a value comparable to the foil thickness ( $\sim 411$  nm). This further indicates that free surfaces should be highly involved in strain relaxation.

All the above real-time observations provide direct and quantitative information about the nature of dislocation emission from the austenite tip with a near Pitch OR. Austenite laths with the near K-S OR and the N-W OR have also been observed growing from ferrite during in-situ heating. Dislocation emission was generally observed from tips of most of these austenite laths with three types of ORs. This implies the strain field due to the transformation of austenite is large enough to cause the nucleation and emission of dislocations from an austenite lath tip. The knowledge of the activated slip systems and the evaluation of the stress field at the tip can be compared to results from phase transformation models. This will be included in our further work.

In summary, dislocation loops were observed to be emitted from the tip of austenite lath newly precipitated from ferrite matrix by in-situ TEM. A detailed analysis has been made on an austenite with a near Pitsch OR, that is  $(100)_f \parallel (110)_b$ ,  $0.6^\circ$  and  $[0\bar{1}1]_f \parallel [1\bar{1}1]_b$ ,  $0.6^\circ$ . The dislocations with the Burgers vector of  $[111]_b/2$  gliding first in  $(11\bar{2})_b$  and then in  $(10\bar{1})_b$  plane were emitted during the tip motion. The jerky nature of the lath speed is associated with the emission of dislocations. The shear stresses in front of the tip can be evaluated using dislocation as stress probes. These quantitative results based on the dislocation analysis provide useful data for revealing the important strain and stress field associated with the interface migration.

Supplementary data to this article can be found online at <https://doi.org/10.1016/j.scriptamat.2017.10.014>.

## Acknowledgements

This work was supported by National Natural Science Foundation of China (no. 51471097 and no. 51671111), National Key Research and Development Program of China (no. 2016YFB0701304) and the Chinese Scholarship Council for funding the stay of Juan Du at CEMES. This work has been supported by the French National Research Agency under the “Investissement d’Avenir” program reference no. ANR-10-EQPX-38-01. Helpful discussions from Professors David Rodney, Long-Qing Chen, Rong Yu, Tong-Yi Zhang, and Xiao-Yan Li are gratefully acknowledged.

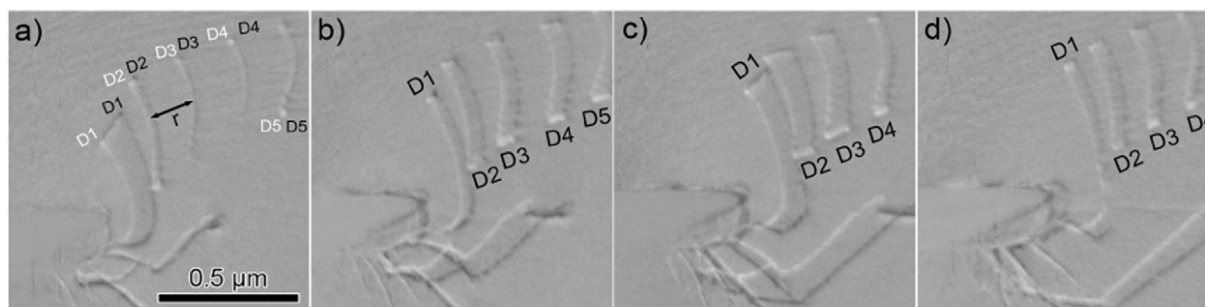


**Fig. 4.** Image differences between snapshots at different time showing the displacements of emitted dislocations, numbered by D1–D5: a) 126.2 s–127.2 s, b) 127.2 s–131.2 s, c) 131.2 s–135.2 s, d) 135.2 s–139.2 s. The dislocations appear white and black before and after, respectively. See Supplementary movie S2 for details.

## References

- [1] J.K. Chen, G. Chen, W.T. Reynolds Jr., *Philos. Mag. A* 78 (2) (1998) 405–422.
- [2] U. Dahmen, P. Ferguson, K. Westmacott, *Acta Metall.* 32 (5) (1984) 803–810.
- [3] C.T. Forwood, L.M. Clarebrough, *Philos. Mag. B* 59 (6) (1989) 637–665.
- [4] T. Furuhashi, K. Wada, T. Maki, *Metall. Mater. Trans. A* 26 (8) (1995) 1971–1978.
- [5] M.G. Hall, H.I. Aaronson, K.R. Kinsma, *Surf. Sci.* 31 (1972) 257–274.
- [6] H. Jiao, M. Aindow, R.C. Pond, *Philos. Mag.* 83 (16) (2003) 1867–1887.
- [7] C.P. Luo, U. Dahmen, *Acta Mater.* 46 (6) (1998) 2063–2081.
- [8] C.P. Luo, G.C. Weatherly, *Acta Metall.* 35 (8) (1987) 1963–1972.
- [9] D. Qiu, W.-Z. Zhang, *Acta Mater.* 56 (9) (2008) 2003–2014.
- [10] W. Bollmann, *Crystal Defects and Crystalline Interfaces*, Springer Science & Business Media, Berlin, 1970.
- [11] W. Bollmann, *Phys. Status Solidi A* 21 (2) (1974) 543–550.
- [12] U. Dahmen, *Scr. Metall.* 15 (1) (1981) 77–81.
- [13] S.Q. Xiao, J.M. Howe, *Acta Mater.* 48 (12) (2000) 3253–3260.
- [14] F. Momprou, J. Wu, W.-Z. Zhang, *Mater. Today Proc.* 2 (2015) S651–S654.
- [15] M. Onink, F.D. Tichelaar, C.M. Brakman, E.J. Mittemeijer, S. Van Der Zwaag, *J. Mater. Sci.* 30 (1995) 6223–6234.
- [16] T. Furuhashi, T. Maki, *Philos. Mag. Lett.* 69 (1) (1994) 31–36.
- [17] G. Chen, G. Spanos, R.A. Masumura, W.T. Reynolds, *Acta Mater.* 53 (4) (2005) 895–906.
- [18] W. Pitsch, *Philos. Mag.* 4 (44) (1959) 577–584.
- [19] J. Douin, P. Veyssière, P. Beauchamp, *Philos. Mag.* 54 (1986) 375–393.